

Supporting Information

Regular and red-shifted fluorescence of the donor-acceptor compound 5-(1H-pyrrol-1-yl)thiophenecarbonitrile (TCN) is efficiently quenched by internal modes of thiophene

Mercedes V. Bohnwagner^a, Irene Burghardt^b, Andreas Dreuw^{a*}

^a Interdisciplinary Center for Scientific Computing, Im Neuenheimer Feld 205, 69120 Heidelberg, Germany. Tel: +49 6221 5414735 ;
E-mail: dreuw@uni-heidelberg.de

^b Institute of Physical and Theoretical Chemistry, Max-von-Laue-Straße 7, 60438 Frankfurt, Germany

Contents:

Table S1. Cartesian coordinates of the S_0 equilibrium geometry of 2-TCN obtained at RI-MP2/cc-pVTZ level of theory.

Table S2. Cartesian coordinates of the S_0 equilibrium geometry of 2-TCN obtained RI-CC2/cc-pVTZ level of theory.

Table S3. Cartesian coordinates of the S_0 equilibrium geometry of 3-TCN obtained at RI-MP2/cc-pVTZ level of theory.

Table S4. Cartesian coordinates of the S_0 equilibrium geometry of 3-TCN obtained at RI-CC2/cc-pVTZ level of theory.

Table S5. Cartesian coordinates of the S_1 ($S(\pi\pi^*)$) equilibrium geometry of 2-TCN obtained at TD-CAM-B3LYP/cc-pVTZ level of theory.

Table S6. Cartesian coordinates of the approximate ring-opened S_1/S_0 conical intersection geometry of 3-TCN obtained at TD-CAM-B3LYP/cc-pVTZ level of theory.

Table S7. Cartesian coordinates of the S_1 ($S(\pi\pi^*)$) equilibrium geometry of 2-TCN obtained at TD-BHLYP/cc-pVTZ level of theory.

Table S8. Cartesian coordinates of the S_1 ($S(\pi\pi^*)$) equilibrium geometry of 3-TCN obtained at TD-BHLYP/cc-pVTZ level of theory.

Table S9. Cartesian coordinates of the S_2 ($S(CT)$) equilibrium geometry of 2-TCN obtained at RI-CC2/cc-pVTZ level of theory.

Table S10. Cartesian coordinates of the S_2 ($S(CT)$) equilibrium geometry of 3-TCN obtained at RI-CC2/cc-pVTZ level of theory.

Table S11. Comparison of vertical excitation energies and static dipole moments of the first two lowest singlet and triplet states of TCN obtained at ADC(2)/cc-pVTZ and ADC(2)/cc-pVTZ/SS-COSMO levels of theory at the gas phase ground state equilibrium geometry using the parameter of n-hexane, acetonitrile and water for the solvent model. Vertical excitation energies in gas phase ω_{ex} (eV), solvent-corrected vertical excitation energies $\omega_{ex,sol}$ (eV), solvent shifts $\Delta\omega_{ex,gas}^a$ and $\Delta\Delta\omega_{ex,sol}^b$ (eV) and relaxed static dipole moments (D) are given.

Figure S1. a) HOMO-1, HOMO, LUMO and LUMO+1 of 2-TCN b) HOMO-1, HOMO, LUMO and LUMO+1 of 3-TCN (bottom) computed at the RI-ADC(2)/cc-pVTZ level at the RI-CC2/cc-pVTZ ground state equilibrium geometry (isovalue = 0.05, 0.0125). DFT/BHLYP MOs are practical identical.

Figure S2. RI-ADC(2)/cc-pVTZ electron detachment (red) and attachment (blue) density plots for the S_1 , S_2 , T_1 and T_2 states of 3-TCN calculated at the RI-CC2 ground state equilibrium geometry. TDDFT/BHLYP electron detachment-attachment densities are practical identical (isovalue = 0.009 and 0.00225).

Figure S3. TDDFT/BHLYP/cc-pVTZ electron detachment (red) and attachment (blue) density plots for the S_1 and S_2 state of 2-TCN obtained at the RI-CC2/cc-pVTZ ground state equilibrium geometry (isovalue = 0.009, 0.002). The density plots for T_1 and T_2 are almost identical to the ADC(2) ones.

Figure S4. The dominant natural transition orbital (NTO) pairs for the S_1 and S_2 state of 2-TCN(a)) and 3-TCN(b)) obtained at the RI-ADC(2)/cc-pVTZ level of theory at the RI-CC2 ground state equilibrium geometry (isovalue = 0.05). For each state, the "hole" is on the left, the "particle" on the right. The associated eigenvalues λ are 0.7925 and 0.8088, respectively.

Figure S5. RI-ADC(2)/cc-pVTZ electron (red) and hole (blue) density plots for the S1 and S2 states of 2-TCN (a) and 3-TCN (b) calculated at the RI-CC2/cc-pVTZ ground state equilibrium geometry (isovalue = 0.015 and 0.005).

Figure S6. S1 state equilibrium geometries of 2-TCN a) and 3-TCN a) obtained at TD-CAM-B3LYP/cc-pVTZ (left) and TD-BHLYP/cc-pVTZ (right) level of theory.

Figure S7. Schematic representation of the deactivation pathway of the S(CT) (S2) state of TCN in acetonitrile. In the SS-COSMO calculation the solvent charges have been equilibrated with respect to the S(CT) state density. Vertical excitation energies of S($\pi\pi^*$) and S(CT) states and the total energies of the S(CT) equilibrium geometries (TICT) (relative to the S0 equilibrium energy) obtained at ADC(2)/cc-pVTZ/SS-COSMO level of theory are given in the table.

Comment: Details about TDDFT geometry optimizations of the S1 state.

Table S1: Cartesian coordinates of the S₀ equilibrium geometry of 2-TCN obtained at RI-MP2/cc-pVTZ level of theory.

S	-0.918723	-0.902058	-0.267189
C	0.222914	0.338137	0.095324
C	-2.231057	0.184142	-0.005544
C	-0.389325	1.541928	0.379145
C	-1.791081	1.456572	0.316242
H	-2.471172	2.270191	0.516682
H	0.165955	2.428205	0.644886
C	-3.567251	-0.265322	-0.111020
N	-4.676457	-0.641546	-0.202430
N	1.588474	0.075342	0.037513
C	2.532495	0.927582	-0.494267
C	2.206955	-1.068715	0.494531
C	3.558782	-0.938444	0.253896
C	3.763667	0.318667	-0.368969
H	2.232438	1.858629	-0.941924
H	4.699716	0.733177	-0.700990
H	1.635497	-1.840150	0.980900
H	4.309420	-1.666258	0.508790

Table S2: Cartesian coordinates of the S_0 equilibrium geometry of 2-TCN obtained RI-CC2/cc-pVTZ level of theory.

S	-4.802297	4.980847	-0.881293
C	-4.799836	5.457621	-2.544259
C	-3.072820	4.867594	-0.879853
C	-3.520092	5.551001	-3.059247
C	-2.536843	5.219669	-2.108261
H	-1.473824	5.208739	-2.298515
H	-3.321588	5.818405	-4.086153
C	-2.382702	4.440427	0.276232
N	-1.807003	4.085299	1.247413
N	-5.996915	5.737746	-3.193626
C	-6.173489	6.739750	-4.132030
C	-7.194142	5.068845	-3.006710
C	-8.131428	5.648076	-3.834624
C	-7.488622	6.701667	-4.542388
H	-5.360432	7.400210	-4.378553
H	-7.936666	7.365382	-5.262148
H	-7.246702	4.225194	-2.339808
H	-9.159196	5.340323	-3.924911

Table S3: Cartesian coordinates of the S_0 equilibrium geometry of 3-TCN obtained at RI-MP2/cc-pVTZ level of theory.

S	0.461614	-1.712654	0.169718
C	-0.123202	-0.100526	-0.030495
C	2.085422	-1.191492	0.108558
C	0.902805	0.812887	-0.114786
C	2.169193	0.182944	-0.028633
H	0.751119	1.871318	-0.257915
H	2.897779	-1.896681	0.161255
N	-1.489822	0.160747	-0.042089
C	-2.093326	1.228391	0.587688
C	-2.447493	-0.599238	-0.678876
C	-3.671468	-0.004523	-0.453817
C	-3.448256	1.146034	0.344024
H	-1.507543	1.914502	1.173696
H	-4.189599	1.834224	0.711391
H	-2.163302	-1.459221	-1.259959
H	-4.614843	-0.359046	-0.831243
C	3.407547	0.880378	-0.101696
N	4.427058	1.458880	-0.160598

Table S4: Cartesian coordinates of the S_0 equilibrium geometry of 3-TCN obtained at RI-CC2/cc-pVTZ level of theory.

S	-4.797803	4.979371	-0.879879
C	-4.805928	5.470395	-2.542992
C	-3.087418	4.888440	-0.859762
C	-3.531978	5.584494	-3.051607
C	-2.548413	5.256062	-2.080153
H	-3.315381	5.861222	-4.072204
H	-2.561208	4.562892	0.022559
N	-6.007983	5.741971	-3.188973
C	-6.200531	6.749589	-4.117440
C	-7.194058	5.053232	-3.007402
C	-8.141802	5.626711	-3.827954
C	-7.515606	6.695425	-4.527196
H	-5.396853	7.422644	-4.360931
H	-7.973881	7.358439	-5.241128
H	-7.233757	4.204657	-2.345926
H	-9.165831	5.306530	-3.917581
C	-1.147324	5.276406	-2.332649
N	0.014939	5.298638	-2.544458

Table S5: Cartesian coordinates of the S_1 ($S(\pi\pi^{**})$) equilibrium geometry of 2-TCN obtained at TD-CAM-B3LYP/cc-pVTZ level of theory.

S	-0.888112	-1.004266	0.315199
C	0.239183	0.340473	0.153452
C	-2.209777	0.143042	0.170232
C	-0.405974	1.598009	0.052942
C	-1.769532	1.483251	0.059215
H	-2.461168	2.305574	-0.017615
H	0.130616	2.528814	-0.021786
C	-3.526649	-0.303869	0.161612
N	-4.617807	-0.687190	0.165692
N	1.561713	0.096633	0.084085
C	2.566973	1.035409	-0.137798
C	2.157642	-1.166147	0.219536
C	3.499169	-1.011271	0.084278
C	3.757508	0.377702	-0.140006
H	2.330485	2.071787	-0.282631
H	4.722156	0.832573	-0.284137
H	1.552969	-2.033549	0.411290
H	4.231851	-1.796897	0.142014

Table S6: Cartesian coordinates of the approximate ring-opened S_1/S_0 conical intersection geometry of 3-TCN obtained at TD-CAM-B3LYP/cc-pVTZ level of theory.

S	1.038888	-2.355605	-0.469668
C	-0.240409	-0.169473	-0.238438
C	2.266481	-1.306453	-0.085423
C	0.833848	0.666846	-0.106938
C	2.110122	0.095898	-0.081567
H	0.746794	1.738571	0.040299
H	3.209847	-1.732958	0.213389
N	-1.517260	0.182686	-0.095016
C	-2.060999	1.430344	0.287284
C	-2.586166	-0.651028	-0.414606
C	-3.738398	0.016453	-0.242715
C	-3.396633	1.348617	0.214453
H	-1.427843	2.247633	0.573260
H	-4.089337	2.129038	0.479107
H	-2.402675	-1.676742	-0.676980
H	-4.725731	-0.368339	-0.422748
C	3.232183	0.943977	0.131846
N	4.137630	1.630507	0.274161

Table S7: Cartesian coordinates of the S_1 ($S(\pi\pi^*)$) equilibrium geometry of 2-TCN obtained at TD-BHLYP/cc-pVTZ level of theory.

S	-4.814010	4.331125	-1.152953
C	-4.804291	5.266173	-2.648090
C	-3.114781	4.713437	-0.957612
C	-3.495749	5.668959	-3.030875
C	-2.560509	5.361145	-2.098230
H	-1.516910	5.588445	-2.169318
H	-3.291649	6.164725	-3.957556
C	-2.459219	4.430464	0.228753
N	-1.919516	4.172833	1.210915
N	-5.957601	5.641140	-3.224450
C	-6.100618	6.559905	-4.254585
C	-7.218873	5.164733	-2.887879
C	-8.126089	5.768265	-3.688532
C	-7.416377	6.648808	-4.556964
H	-5.253553	7.068935	-4.654339
H	-7.839708	7.273178	-5.314670
H	-7.333263	4.431704	-2.120192
H	-9.181917	5.602863	-3.672184

Table S8: Cartesian coordinates of the S_1 ($S(\pi\pi^*)$) equilibrium geometry of 3-TCN obtained at TD-BHLYP/cc-pVTZ level of theory.

S	-4.784905	4.356721	-1.065046
C	-4.814657	5.209799	-2.678398
C	-3.160231	4.835059	-0.909361
C	-3.517314	5.516071	-3.101669
C	-2.563355	5.232695	-2.150962
H	-3.300866	5.918970	-4.070645
H	-2.720544	4.987742	0.056064
N	-5.969770	5.634891	-3.221999
C	-6.122230	6.645343	-4.158959
C	-7.222040	5.097545	-2.953995
C	-8.129544	5.743016	-3.710649
C	-7.428497	6.723497	-4.482915
H	-5.281090	7.215295	-4.483905
H	-7.858010	7.405296	-5.185432
H	-7.325845	4.295213	-2.257249
H	-9.180971	5.552129	-3.727713
C	-1.179079	5.405702	-2.330669
N	-0.051876	5.562142	-2.442180

Table S9: Cartesian coordinates of the S_2 ($S(CT)$) equilibrium geometry of 2-TCN obtained at RI-CC2/cc-pVTZ level of theory.

S	-4.821582	4.750520	-0.879139
C	-4.948224	4.429686	-2.635489
C	-3.107351	5.200611	-0.995842
C	-3.667621	4.757840	-3.235103
C	-2.682688	5.120394	-2.338801
H	-1.653964	5.319914	-2.611955
H	-3.507499	4.672961	-4.303669
C	-2.346540	5.486627	0.139851
N	-1.715071	5.740705	1.118250
N	-6.063014	5.237682	-3.202760
C	-6.103445	6.616256	-3.211438
C	-7.190787	4.782532	-3.733110
C	-8.019272	5.909669	-4.127986
C	-7.329348	7.046784	-3.793534
H	-5.264720	7.164025	-2.805190
H	-7.630791	8.071664	-3.933984
H	-7.363897	3.719421	-3.805802
H	-8.988799	5.829527	-4.593043

Table S10: Cartesian coordinates of the S₂ (S(CT)) equilibrium geometry of 3-TCN obtained at RI-CC2/cc-pVTZ level of theory.

S	-4.788492	5.113236	-0.764447
C	-4.934113	4.536849	-2.462580
C	-3.107415	5.582257	-0.951461
C	-3.661429	4.786082	-3.109783
C	-2.683013	5.312163	-2.254800
H	-3.473726	4.538963	-4.147487
H	-2.509456	5.905503	-0.113977
N	-6.054988	5.280635	-3.126241
C	-6.069918	6.640149	-3.347931
C	-7.206347	4.775365	-3.550382
C	-8.025866	5.846609	-4.093155
C	-7.305137	7.004977	-3.957726
H	-5.207622	7.223979	-3.058138
H	-7.590232	8.002279	-4.249486
H	-7.398990	3.717434	-3.455392
H	-9.009191	5.717835	-4.516341
C	-1.344191	5.564382	-2.674858
N	-0.240707	5.788438	-3.041500

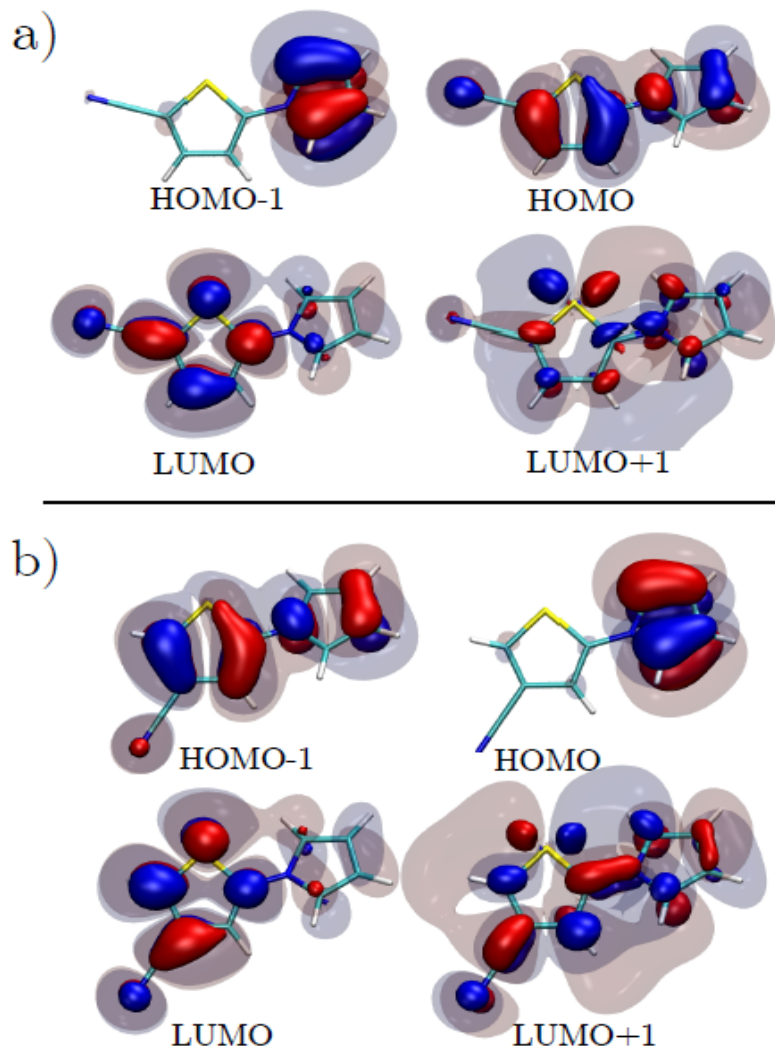


Figure S1: a) HOMO-1, HOMO, LUMO and LUMO+1 of 2-TCN
b) HOMO-1, HOMO, LUMO and LUMO+1 of 3-TCN (bottom)
computed at the RI-ADC(2)/cc-pVTZ level at the RI-CC2/cc-pVTZ
ground state equilibrium geometry (isovalue = 0.05, 0.0125).
DFT/BHLYP MOs are practical identical.

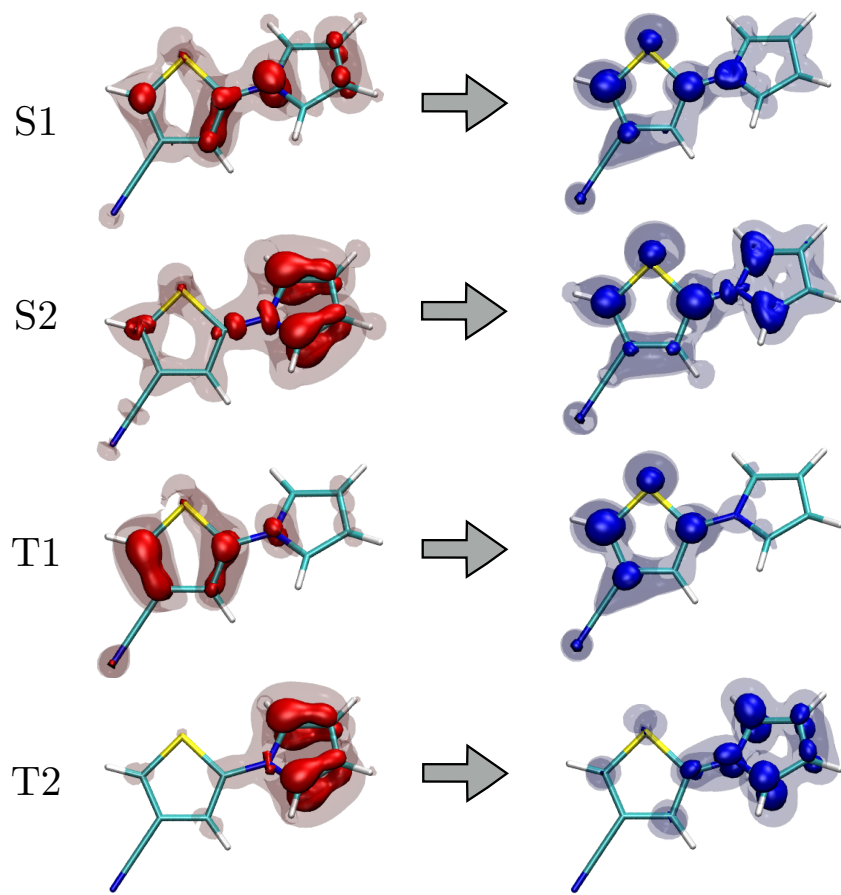


Figure S2: RI-ADC(2)/cc-pVTZ electron detachment (red) and attachment (blue) density plots for the S1, S2, T1 and T2 states of 3-TCN calculated at the RI-CC2 ground state equilibrium geometry. TDDFT/BHLYP electron detachment-attachment densities are practical identical (isovalue = 0.009 and 0.00225).

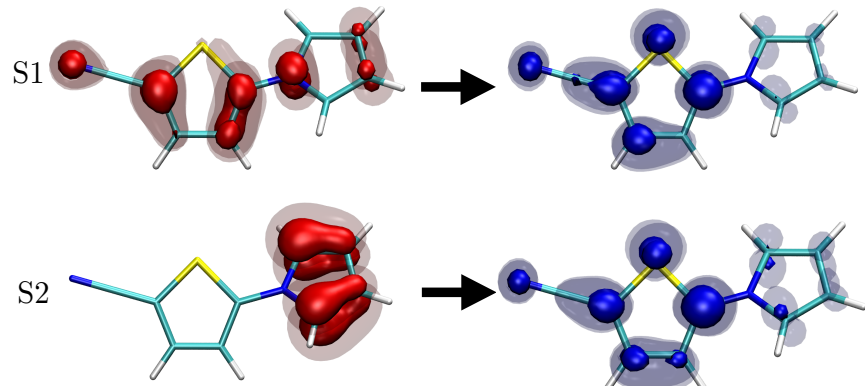


Figure S3: TDDFT/BHLYP/cc-pVTZ electron detachment (red) and attachment (blue) density plots for the S1 and S2 state of 2-TCN obtained at the RI-CC2/cc-pVTZ ground state equilibrium geometry (isovalue = 0.009, 0.002). The density plots for T1 and T2 are almost identical to the ADC(2) ones.

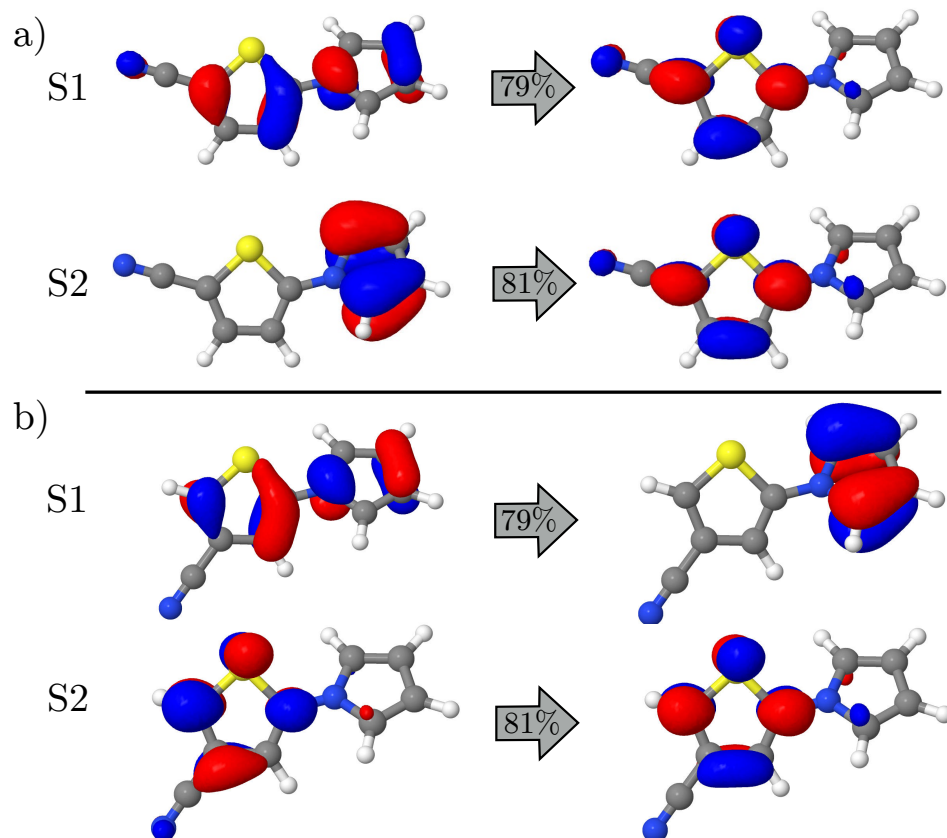


Figure S4: The dominant natural transition orbital (NTO) pairs for the S1 and S2 state of 2-TCN (a)) and 3-TCN (b)) obtained at the RI-ADC(2)/cc-pVTZ level of theory at the RI-CC2 ground state equilibrium geometry (isovalue = 0.05). For each state, the "hole" is on the left, the "particle" on the right. The associated eigenvalues λ are 0.7925 and 0.8088, respectively.

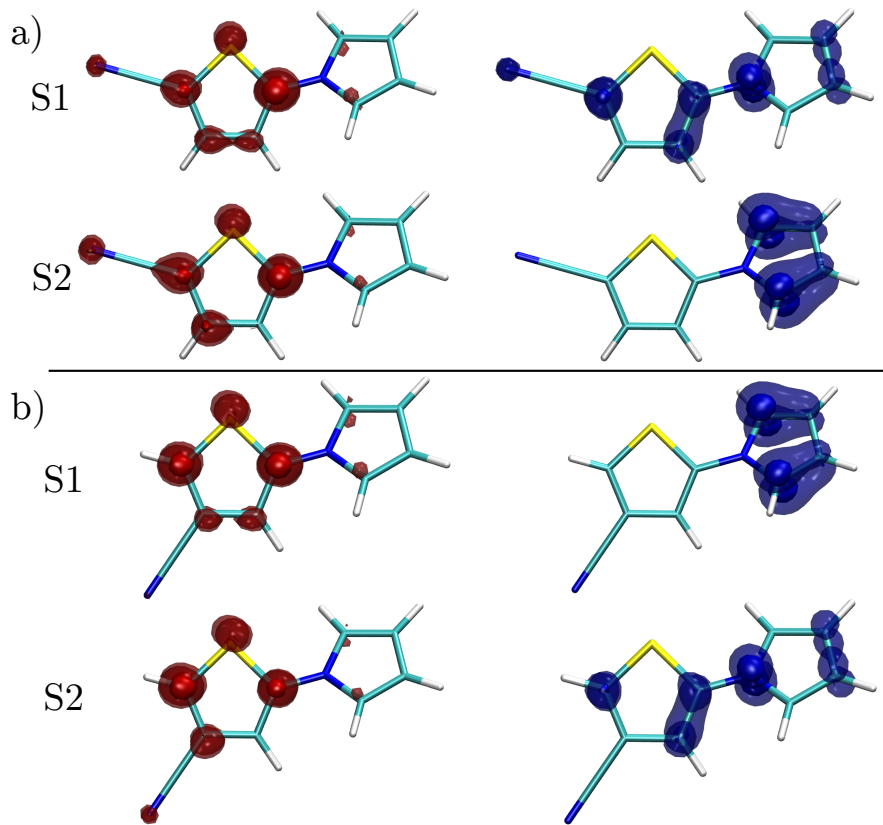


Figure S5: RI-ADC(2)/cc-pVTZ electron (red) and hole (blue) density plots for the S1 and S2 states of 2-TCN (a) and 3-TCN (b) calculated at the RI-CC2/cc-pVTZ ground state equilibrium geometry (isovalue = 0.015 and 0.005).

TDDFT geometry optimizations of the S($\pi\pi^*$) (S1) state

In contrast to RI-CC2, geometry optimizations of the bright S($\pi\pi^*$) (S1) state of 2-TCN performed at TDDFT/BHLYP/cc-pVTZ and TDDFT/CAM-B3LYP/cc-pVTZ levels of theory, converge to stationary points (Figure S6). The minimum has been verified by vibrational frequency analysis at TDDFT/CAM-B3LYP/cc-pVTZ level of theory. Hence, in the case of 2-TCN, TDDFT does not predict an ultrafast deactivation of the bright S($\pi\pi^*$) state via a conical intersection with the ground state. However, this failure of TDDFT is not entirely surprising because it is known that TDDFT tend to fail to describe conical intersections between excited states and the ground state.^{1,2} Interestingly, in the case of the 3-TCN isomer, in contrast to TD-BHLYP, TD-CAM-B3LYP predicts an intersection with the ground state in agreement with RI-CC2.

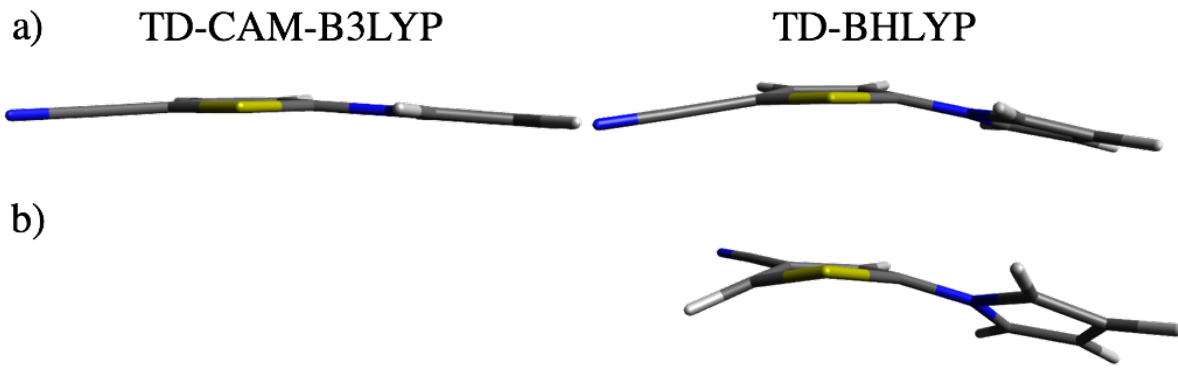


Figure S6: S1 state equilibrium geometries of 2-TCN a) and 3-TCN b) obtained at TD-CAM-B3LYP/cc-pVTZ (left) and TD-BHLYP/cc-pVTZ (right) level of theory.

Table S11: Comparison of vertical excitation energies and static dipole moments of the first two lowest singlet and triplet states of TCN obtained at ADC(2)/cc-pVTZ and ADC(2)/cc-pVTZ/SS-COSMO levels of theory at the gas phase ground state equilibrium geometry using the parameter of n-hexane, acetonitrile and water for the solvent model. Vertical excitation energies in gas phase ω_{ex} (eV), solvent-corrected vertical excitation energies $\omega_{\text{ex,sol}}$ (eV), solvent shifts $\Delta\omega_{\text{ex,gas}}^{\text{a}}$ and $\Delta\Delta\omega_{\text{ex,sol}}^{\text{b}}$ (eV) and relaxed static dipole moments (D) are given.

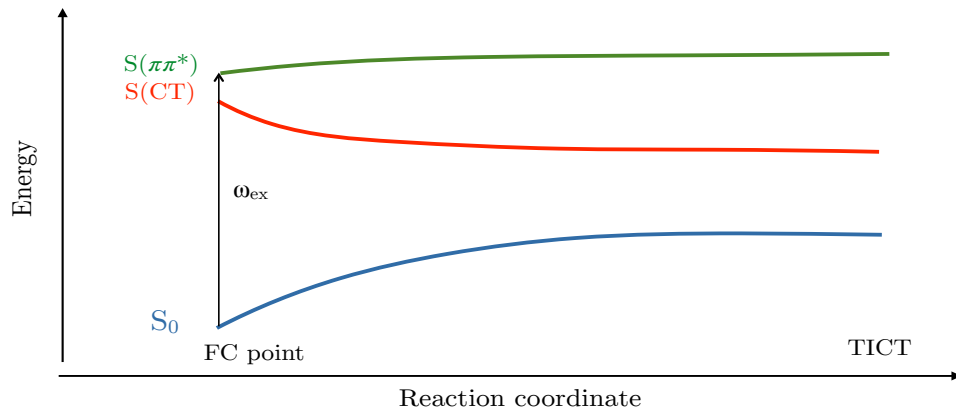
SS-COSMO n-hexane										
State	ω_{ex}	$\omega_{\text{ex,sol}} @ S0$	$\Delta\omega_{\text{ex,gas}}$	μ	$\omega_{\text{ex,sol}} @ S(\pi\pi^*)$	$\Delta\Delta\omega_{\text{ex,sol}}$	μ	$\omega_{\text{ex,sol}} @ S(\text{CT})$	$\Delta\Delta\omega_{\text{sol}}$	μ
2-TCN										
T($\pi\pi^*$)	3.28	3.28	0.00	5.4	3.27	-0.01	6.4	3.28	0.00	7.6
T(CT)	4.01	3.97	-0.04	9.2	3.95	-0.02	10.8	3.93	-0.04	12.8
S($\pi\pi^*$)	4.46	4.34	-0.12	9.3	4.32	-0.02	10.8	4.30	-0.04	13.8
S(CT)	4.88	4.64	-0.24	15.7	4.59	-0.05	16.9	4.55	-0.09	18.0
3-TCN										
T($\pi\pi^*$)	3.51	3.51	0.00	4.7	3.51	0.00	5.9	3.51	0.00	7.0
T(CT)	4.13	4.12	-0.01	7.1	4.10	-0.02	8.5	4.09	-0.03	10.0
S($\pi\pi^*$)	4.75	4.64	-0.11	8.9	4.60	-0.04	10.7	4.59	-0.05	12.1
S(CT)	5.12	4.92	-0.20	13.8	4.85	-0.07	15.6	4.81	-0.11	16.7
SS-COSMO acetonitrile										
2-TCN										
T($\pi\pi^*$)	3.28	3.29	+0.01	6.1	3.18	-0.11	10.5	3.10	-0.19	14.6
T(CT)	4.01	3.99	-0.02	9.9	3.56	-0.43	16.3	3.10	-0.89	20.5
S($\pi\pi^*$)	4.46	4.34	-0.12	10.1	3.96	-0.38	15.3	3.62	-0.72	18.5
S(CT)	4.88	4.67	-0.21	16.4	3.95	-0.72	20.5	3.32	-1.35	22.6
3-TCN										
T($\pi\pi^*$)	3.51	3.53	+0.02	5.2	3.34	-0.19	10.6	3.20	-0.33	14.4
T(CT)	4.13	4.17	+0.04	7.3	3.78	-0.39	14.3	3.33	-0.84	19.1
S($\pi\pi^*$)	4.75	4.65	-0.10	9.4	4.12	-0.53	15.6	3.77	-0.88	18.5
S(CT)	5.12	5.03	-0.09	13.5	4.11	-0.92	19.2	3.51	-1.52	21.8
SS-COSMO water										
2-TCN										
T($\pi\pi^*$)	3.28	3.29	+0.01	6.2	3.18	-0.11	10.6	3.04	-0.25	15.0
T(CT)	4.01	4.00	-0.01	10.0	3.53	-0.47	16.5	3.01	-0.99	20.8
S($\pi\pi^*$)	4.46	4.34	-0.12	10.1	3.94	-0.40	15.5	3.59	-0.75	18.7
S(CT)	4.88	4.68	-0.20	16.4	3.91	-0.77	20.6	3.26	-1.42	22.8
3-TCN										
T($\pi\pi^*$)	3.51	3.53	+0.02	5.2	3.32	-0.21	10.8	3.17	-0.36	15.2
T(CT)	4.13	4.18	+0.05	7.3	3.75	-0.43	14.6	3.27	-0.91	19.0
S($\pi\pi^*$)	4.75	4.65	-0.10	9.5	4.09	-0.56	15.8	3.72	-0.93	18.7
S(CT)	5.12	5.04	-0.08	13.4	4.07	-0.97	20.1	3.45	-1.59	22.0

a $\Delta\omega_{\text{ex,gas}}$ is the difference between vertical excitation energies in gas phase and computed using SS-COSMO equilibrating the screening charge of the solvent with the ground state density

b $\Delta\Delta\omega_{\text{ex,sol}}$ is the difference between vertical excitation energies in solution within COSMO solvation when the screening charge of the solvent is equilibrated with the ground state density and with the respective excited state density

c relaxed convergence criteria have been used due to convergence problems

AN COSMO SOLUTION



	$\omega_{\text{ex}} (\text{S}(\pi\pi^*)) [\text{eV}]$	$\omega_{\text{ex}} (\text{S(CT)}) [\text{eV}]$	$E_{\text{rel}}(\text{TICT}) [\text{eV}]$
2-TCN	3.63	3.32	2.73
3-TCN	3.77	3.51	3.06

Figure S7: Schematic representation of the deactivation pathway of the S(CT) (S2) state of TCN in acetonitrile. In the SS-COSMO calculation the solvent charges have been equilibrated with respect to the S(CT) state density. Vertical excitation energies of S($\pi\pi^*$) and S(CT) states and the total energies of the S(CT) equilibrium geometries (TICT) (relative to the S0 equilibrium energy) obtained at ADC(2)/cc-pVTZ/SS-COSMO level of theory are given in the table.

References

- [1] Handy, N. C.; Cohen, A. J. *Mol. Phys.* **2001**, *99*, 403.
- [2] Levine, B. G.; Queeneville C. Ko, J.; Martínez, T. J. *Molec. Phys.* **2006**, *104*, 1039.